

**CLAY HYDRATION MECHANISMS
AND THEIR EFFECT ON DUSTINESS**

A. LÓPEZ-LILAO¹; M. P. GÓMEZ-TENA¹; G. MALLOL¹; E. MONFORT¹

¹Instituto de Tecnología Cerámica. Asociación de Investigación de las Industrias Cerámicas.
Universitat Jaume I. Castellón. Spain.

Corresponding author: A. López-Lilao

e-mail: ana.lopez@itc.uji.es

Phone: 34 964 34 24 24

Fax: 34 964 34 24 25

Address: ITC Campus Riu Sec 12006 Castellón. Spain

Abstract

Clays are employed in a wide variety of industries such as ceramic industry, manufacture of paper, rubber, etc. In this sense, it is well known that at industrial processes in which clayey materials are used, such as ceramic industry, in order to carry out some specific stages, the wetting of clays is required. Moreover, it is also long established that wetting is an appropriated measure to reduce particulate matter emissions during clays storage and handling.

The present study was undertaken to assess the influence of moisture on clay dustiness because, though the complex behaviour of the clay–water system has been known since antiquity, the mechanisms involved in clay hydration and their influence on dustiness are still not well understood. To encompass a wide range of specific surface areas, three clays and a kaolin were studied. Chemical and mineralogical analysis of these four raw materials was performed and their particle size distribution, flowability, true density, plastic limit, and specific surface area were determined. Raw materials dustiness was determined using the continuous drop method.

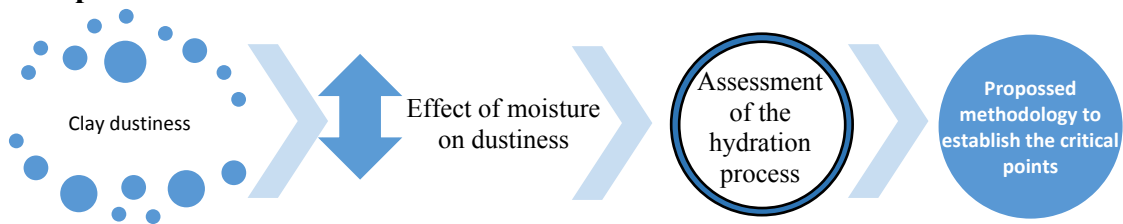
As against what might intuitively be expected, the results showed that the relationship between moisture and dustiness was quite complex and strongly related to the hydration mechanisms. In this regard, to better understand the phenomena involved in the clay hydration process, a specific methodology was developed to estimate the critical points of the clay hydration process (regarding dustiness). This methodology can be readily applied to other clays or even to materials of different nature to predict the optimum moisture and, therefore, it could be employed to propose specific measures which could entail an improvement of outdoor and indoor air quality.

Keywords: clays, moisture, dustiness, hydration mechanisms

Highlights

- Evaluation of the effect of moisture on clay dustiness
- Assessment of the relationship between dustiness and clay hydration mechanisms
- Development of a methodology to establish the critical points in clay hydration

Graphical abstract



1.

Introduction

1.1 Dust generation associated with clay use

Clays are used in a wide variety of industries, such as the ceramics, paper, rubber, and absorbent industries (Mukherjee and Ghosh, 2013). A vast number of workers are thus potentially exposed to particulate matter emitted from dry mechanical processes such as screening and grinding and clay handling and transfer operations (Mukherjee and Ghosh, 2013).

Some industrial activities, such as ceramics manufacture (floor and wall tiles, sanitary ware, tableware, ceramic refractories, etc.) and cement manufacture (grey and white Portland cement, concrete, etc.), are particularly at issue, as many of these industrial goods are clay-based. The raw materials mixture used in manufacturing these products includes considerable amounts of clay, which play a vital part in the different manufacturing process stages. By way of example, figure 1 presents a break-down of the use of national clays in Spain (8.5 million tonnes) in 2012. About 86% of these clays were used in the ceramic industry, 10% in cement manufacture, and 4% in other industries.

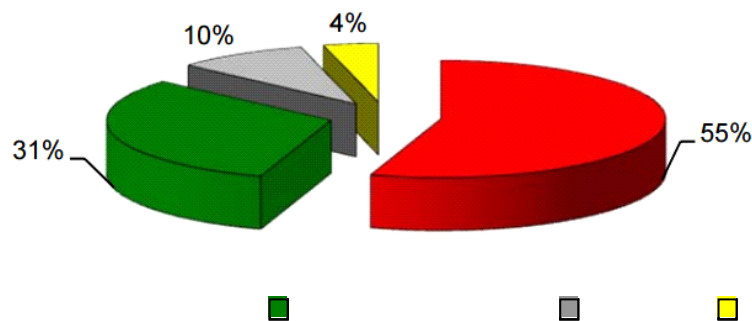


Figure 1. Use of national clays in Spain, 2012. (Instituto Geológico y Minero de España, IGME)

A parameter of great interest in evaluating, controlling, and minimising the risks associated with the particulate matter emissions generated during clay handling is clay dustiness, i.e. clay

tendency to produce dust when handled. In this regard, as the resulting dustiness depends on the apparatus used, standard EN 15051:2013 proposes two test methods: the rotating drum method and the continuous drop method. The test enables the mass fractions of inhalable dust (w_I), thoracic dust (w_T), and respirable dust (w_R) to be determined. The test results allow the materials to be classified in different categories as a function of their dustiness, according to the criteria laid down in the above standard.

1.2 Water as dust suppressor

It is long established that moisture content increases the interparticle binding forces, which leads to less dust generation (WHO/SDE/OEH/99.14). Dustiness was observed to decrease with increasing moisture content in different experimental and observational field studies in which water was added to dusty solids to reduce their dustiness (Alwis et al., 1999; Farrugia et al., 1989; Hjemsted and Schneider, 1996; Plinke et al., 1992; Teschke et al., 1999; Westborg and Cortsen, 1990). Industrial examples of the use of water as a dust suppressor include using water as a wetting agent in the bulk outdoor storage of certain dusty materials, wet processing of minerals, and the use of slurries and wetted materials in the ceramic industry (WHO/SDE/OEH/99.14). Water is the most common dust suppressor because of its availability, low cost, and chemical compatibility.

However, other studies (Cowherd et al., 1989; Plinke et al., 1995) found that the dustiness index of some materials rose when moisture content increased slightly, dustiness subsequently decreasing when moisture content was further raised.

Moisture may therefore be considered to have a rather complex effect, which may vary from one material to another, depending on the extent to which water is absorbed internally or is

attached to the particle surface (Leith D. 1991). That is, its effect depends on the material and on the material's surface properties and hygroscopicity (WHO/SDE/OEH/99.14).

1.3 Clay hydration mechanisms

In order to understand the effect of moisture on clays dustiness, it is needed to know the mechanisms involved in the hydration of clays. Clay water retention takes place by two mechanisms: adsorption and capillary condensation, and the following domains may be distinguished (Prost et al., 1998):

Domain 1: In this adsorption domain, **water is first adsorbed on the material's hydrophilic sites** (exchangeable cations, edge cations, and surface OH groups). It can induce the creation of pillars between clay layers, expanding the layers (interlamellar swelling) and eventually, results in a creation of a film of water on surfaces. Capillary condensation at contact points between particles may also occur in this domain.

Domain 2: Multilayer adsorption then occurs on "free surfaces", which are either unsaturated pore walls or surfaces of layers or particles that can expand freely. This does not necessarily mean that the entire water structure adsorbed by this process is affected by the surface: only about 2–3 layers of adsorbed water are perturbed by clay surfaces (Prost et al., 1998; Revil and Lu, 2013).

In this regard, Hagamassy (1970) obtained the statistical number of water layers versus relative pressure (P/P_0) for a wide variety of non-porous adsorbents. Hagamassy classified the obtained results in different groups based on the heat of adsorption of water on the adsorbents, to this regard each group was characterised by its BET constant (C), which is an index linked with the affinity between adsorbate and adsorbent. Hagamassy results can be summarised as follows: for low relative pressures ($P/P_0 < 0.5$) four groups were established ($C=5.2$, $C=10-14.5$, $C=23$, $C=50-200$), whilst for high relative pressures ($P/P_0 > 0.5$) two groups were

distinguished ($C=5.2$ and $C=10-200$) The C values obtained in our study were in the range 6.9-7.2 and, therefore, the results obtained by Hagamassy for the group with $C=5.2$ have been considered the most appropriated for all the range of relative pressures. Ormerod and Newman (1983) and Moore et al. (2007) postulated that water sorption on the external surfaces of clays was similar to that on reference non-porous oxides (Hagamassy, 1970), so that the relation between relative pressure and the statistical water layers may also be assumed to be valid for porous materials.

Table 1: Statistical water layers versus relative pressure using the procedure proposed by Hagamassy ($C= 5.2$)

Relative pressure P/P_0 (%)	Water layers
0.35	1
0.73	2
0.90	3
0.95	4
0.98	5
1.00	6

Domain 3: In this domain, capillary condensation of water in pores must be involved (Benchara 1991; Carott et al., 1982; Prost et al., 1998). The capillary condensation phenomenon occurs in pores that correspond to the fabric of hydrated particles.

As the amount of water increases, the added water is attracted by the water already adsorbed at the solid surface by the cohesion forces while tending to minimise the water–air interface area, so that particles start to be held together by liquid bridges at their contact points (**pendular state**). If more water is added, some pores become fully saturated by liquid, while

air-filled voids still remain (**funicular state**). Note that the transition between the pendular and the funicular state (5% saturation degree) entails about a threefold increase in granule tensile strength from the pendular state (Oliva, 2015). Water then starts to fill the interparticle voids until all these voids are filled with liquid, but the surface liquid is drawn back into the pores under capillary action (capillary state).

Domain 4: This domain is related to the multilayer adsorption process on grain or particle "free surfaces" and to a capillary condensation mechanism in saturated pores whose size increases or decreases as swelling or shrinkage occurs. Finally, particles are fully immersed in liquid (**slurry state**).

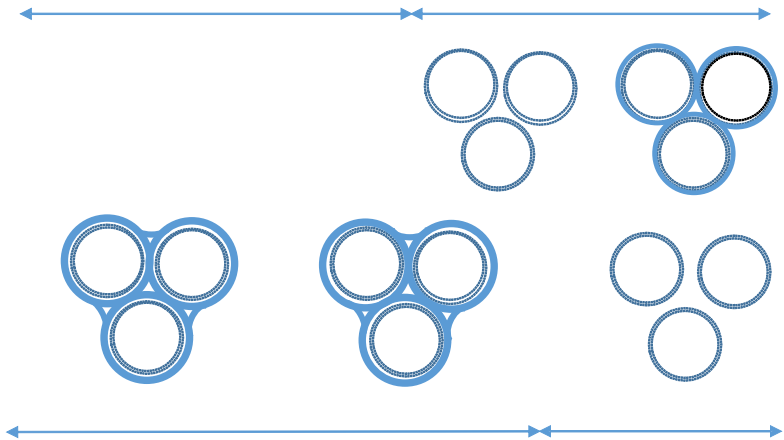


Figure 2. Scheme of the hydration process

In view of these mechanisms, these stages may reasonably be assumed to influence interparticle attractive forces and therefore clay particle cohesion and dustiness. To identify these mechanisms and their effect on dustiness, the identification of the critical points was deemed crucial. However, no clear and compressive methodology to experimentally determine and quantify these critical points was found in the reviewed literature.

2 Objective and scope

Though water is the main dust suppressor in the use of clays in industrial practice and the complex behaviour of the clay–water system has been known since antiquity, the clay hydration mechanisms and their influence on dustiness are still not well understood. This study was therefore undertaken with the following objectives:

- To evaluate the effect of moisture on clay dustiness.
- To develop a methodology to establish the critical points in clay hydration.
- To analyse the relationship between dustiness and the clay hydration mechanisms.

As the effect of moisture depends on the extent to which water is adsorbed, the study was conducted on four clays that encompassed a wide range of specific surface areas (12–33 m²/g). Many industrial clays may therefore be assumed to behave like the studied raw materials. Moreover, the relationship found between hydration mechanisms and dustiness could help to predict or comprehend the effect of moisture on other clays or even on materials of different nature, and this information could be deemed to be essential in order to propose specific preventive measures, which could entail an improvement of air quality and in occupational health when clays are industrially processed.

3 Materials used and experimental procedure

3.1 Raw materials used

The study was conducted on three clays and a kaolin, selected to encompass a wide range of specific surface areas. The main characteristics of these raw materials were determined: chemical analysis (table 2); mineralogical analysis (table 3 and table 4); particle size distribution by laser diffraction measurements (figure 2); true density and specific surface area (table 5). The procedures used in these characterisations are set out in point 3.2.

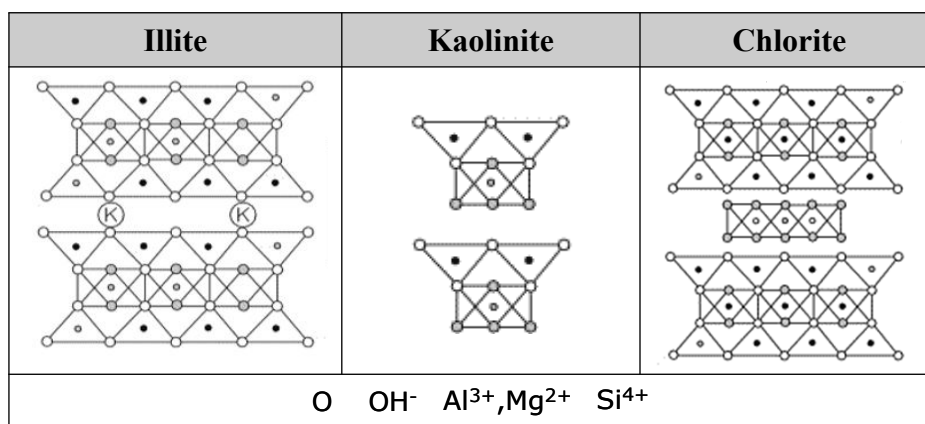
Table 2. Chemical analysis and loss on ignition (L.O.I.) of the selected raw materials (% by weight)

Oxides	Raw materials			
	Clays			Kaolin
	C1	C2	C3	K1
SiO ₂	60.2	57.5	75.3	49.2
Al ₂ O ₃	19.2	21.9	26.9	36.8
CaO	1.79	7.66	0.25	0.02
MgO	0.84	0.62	0.58	0.24
K ₂ O	4.95	1.44	2.47	1.16
Na ₂ O	0.35	0.44	0.54	0.08
Fe ₂ O ₃	7.69	3.55	0.94	0.75
TiO ₂	0.85	1.09	1.38	0.11
L.O.I.	4.6	6.3	7.6	12.3

Table 3. Mineralogical analysis of the selected raw materials (% by weight)

Crystalline phases	Raw materials			
	Clays			Kaolin
	C1	C2	C3	K1
Kaolinite	18	19	59	80
Chlorite	-	-	-	5
Illite	26	22	4	9
Quartz	42	39	33	6
Carbonates	4	3	-	-
Feldspars	2	8	-	-
Fe and Ti compounds	7	7	-	-
Others	1	2	5	-

Table 4. Crystalline structure of the identified phyllosilicates



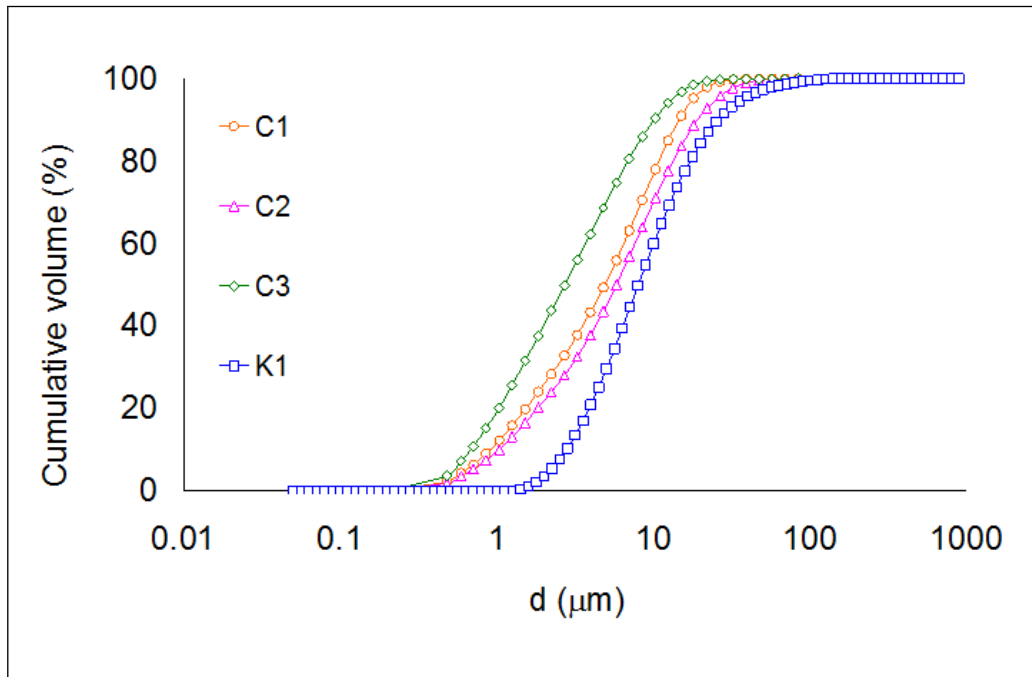


Figure 3. Particle size distribution of the studied raw materials

Table 5. True density and specific surface area of the studied raw materials

	Raw materials			
	Clays			Kaolin
	C1	C2	C3	K1
True density (kg/m ³)	2630	2630	2610	2610
Specific surface area (m ² /g)	14	33	30	12

To evaluate the influence of moisture on dustiness and to cover a wide moisture range (0.05–14%), twenty-seven test samples were prepared by respective wetting of the four studied raw materials.

3.2 Experimental procedure

The methodology followed can be divided into three parts: physic-chemical characterisation of the raw materials, physical characterisation of the bulk samples (dry and wet samples), and identification of the critical points in the clay hydration process.

3.2.1 Physic-chemical characterisation of the raw materials

Raw materials **chemical analysis** (table 2) was carried out by wavelength dispersive X-ray fluorescence spectrometry (WD-XRF model Axios Panalytical) using reference materials to guarantee measurement traceability. Loss on ignition at 1000°C was carried out using a LECO model TGA-701 thermogravimetric analyser.

Mineralogical characterisation (table 3) was performed by XRD quantitative mineral analysis. A Bruker Theta-Theta D8 Advance diffractometer was used for this purpose. The samples were ground to a particle size of less than 40 µm. Readings were taken at 2θ intervals between 5° and 90°. TOPAS software was used to perform Rietveld quantitative analysis.

Particle size distribution (PSD) (figure 2) was determined by laser diffraction (ISO 13320 - 1), using the wet method, i.e. solid samples were dispersed in water, which acted as a dispersion medium.

Specific surface area (table 5) was obtained by nitrogen adsorption according to the BET method (ISO 9277).

True density (table 5) was determined using a helium pycnometer (Quantachrome) (ISO 18753:2004). The technique is based on the determination of the true volume that the powder occupies by means of the difference between the cell volume and the volume that the helium occupies that is introduced to complete cell filling. True density is calculated based on the mass of the powder used. The cell used for the density determination had a volume of 135 cm³.

3.2.2 Characterisation of the bulk samples

In view of the authors' experience in previous dustiness studies (López-Lilao et al., 2015; López-Lilao et al., 2016), apart from the dustiness test, the determination of bulk sample flowability was considered essential to better understand the results. The methodology used to

determine these parameters is briefly described below.

Hausner ratio

The flowability of the particulate samples was evaluated by determining the Hausner ratio (HR), i.e. the quotient of the bulk density of the packed particle bed (by vibration or tapping) and the aerated bulk density of the particle bed (Mallol et al., 2008). The Hausner ratio allowed the materials to be classified as a function of their flowability, as detailed in table 6.

Table 6: Classification of the materials as a function of their Hausner ratio

Hausner ratio	Material behaviour
$HR > 1.40$	Cohesive
$1.4 > HR > 1.25$	Easy flow
$1 > HR > 1.25$	Free flow

Dustiness test

According to standard EN 15051:2013, users need to choose the reference test method that most appropriately simulates their materials and handling processes. In this study, the tests were conducted using the continuous drop method, as this was deemed to adequately simulate the most significant dusty loading and unloading operations in the ceramic and related industries (IPTs, 2006), such as the loading and unloading of ships, trucks, and wagons, and conveyor belt, silo, and hopper discharges. The sampling apparatus (figure 4) consisted, basically, of a cylindrical pipe through which air circulated in an upward direction at a volume flow rate of 53 l/min. The test material was dropped from the top of this pipe at a rate of 6 to 10 g/min. The dust dropped through an inner pipe, concentric to the pipe through which the air rose. This tube was shorter than the outer pipe, so that the dust was released into a counter-current airflow. A pair of sampling heads for health-relevant particle size fractions were located slightly above the discharge position of the material, enabling the inhalable and

the respirable fractions to be studied simultaneously. The inhalable fraction represented the mass fraction of total airborne particles which is inhaled through the nose and mouth, whereas the respirable fraction represented the mass fraction of inhaled particles penetrating to the unciliated airways (EN 481:1995).

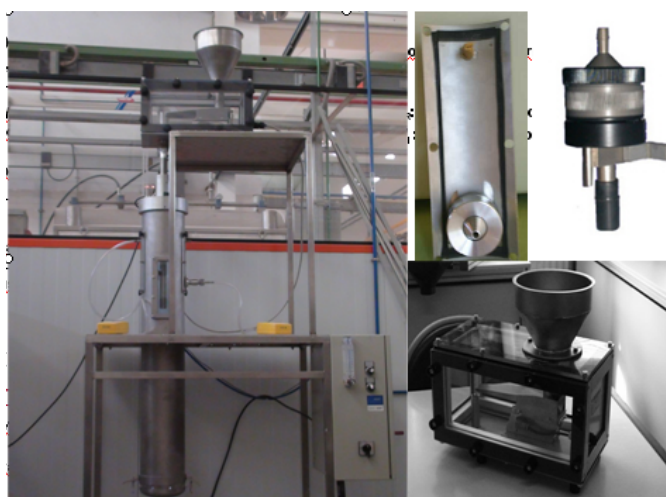


Figure 4. Dustiness tester used and detail of the feeder and sampling heads

In addition, the results obtained allowed the materials to be classified in different categories as a function of their dustiness, according to the criteria laid down in the above standard (table 7).

Table 7: Dustiness classification according to standard UNE EN 15051:2013

Method	Classification	Mass fraction of dust (mg/kg)	
		^{A)} w _I	^{A)} w _R
Method B Continuous drop method	Very low	<1000	<20
	Low	1000 to 4000	20 to 70
	Moderate	4000 to 15000	70 to 300
	High	>15000	>300

^{A)} w_I, w_R: Inhalable and respirable mass fractions, respectively

3.2.3 Methodologies to identify critical stages or points

As mentioned above, no clear and compressive methodology to experimentally determine and quantify the critical points in clay hydration were found in the reviewed literature. An experimental methodology, based on three experimental determinations (moisture adsorption isotherm, saturation degree, and plastic limit), was therefore developed for this study. This methodology and its relationship with the domains described in the introduction are summarised in figure 5.

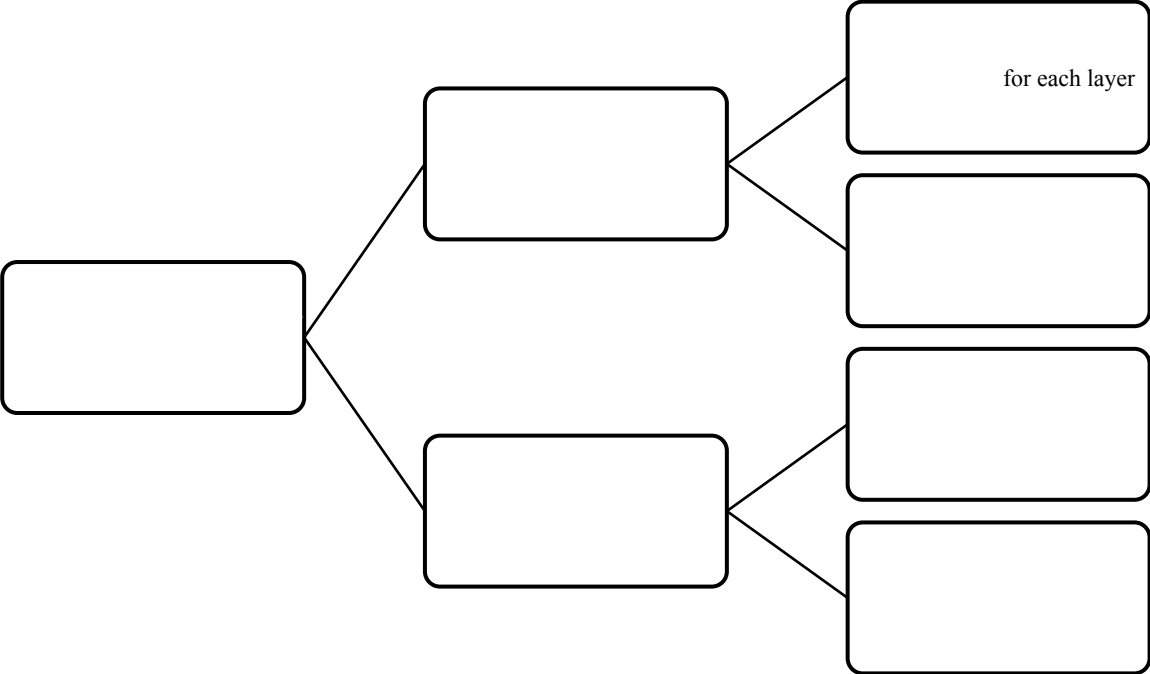


Figure 5. Methodology developed to obtain the critical points

Moisture adsorption isotherm

The water adsorption isotherms of the clays were determined in a DVS Aquadyne Quantachrome instrument using water vapour as adsorbent. The amount of adsorbed water vapour was measured by a static gravimetric method, obtaining moisture gain values depending on the relative humidity. For each relative humidity, equilibrium was reached. The isotherms were obtained at room temperature.

Saturation degree

The saturation degree is the ratio of the liquid volume (V_w) to the total void volume (V_v) in a porous material.

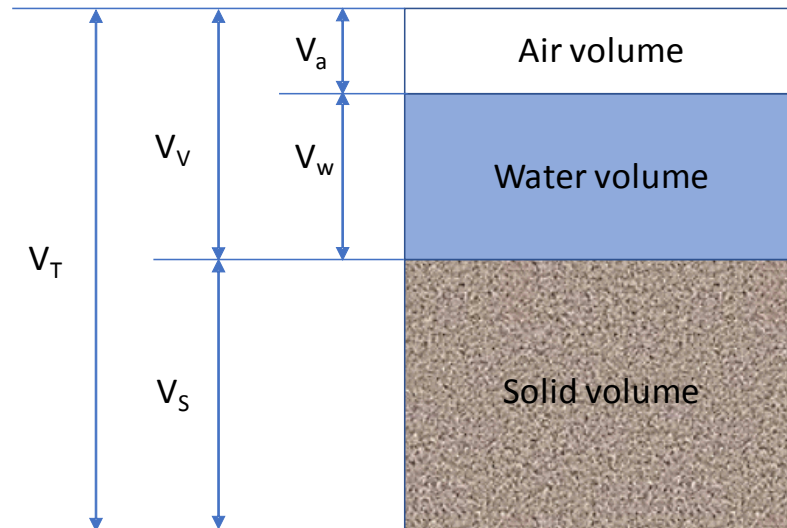


Figure 6. Scheme of the saturation degree concepts: V_T : total volume, V_v : void volume, V_a : air volume, V_w : water volume, V_s : solid volume

The saturation degree was obtained from the ratio of free water volume to void volume (equation 1), void volume being determined from the true density and the aerated bulk density of the particle bed (equation 2).

Equation 1

In this study, in order to estimate bound water, the water volume associated with the three adsorbed layers perturbed by the clay surface was determined (equations 2 and 3) from the specific surface area and the thickness of three water molecules (0.9 nm).

Equation 2

Equation 3

According to Oliva (2015), the transition between the pendular and the funicular state (critical point E) lies at 5% saturation degree. The moisture at which this saturation degree was reached was therefore determined.

Plastic limit

In the proposed methodology, the dustiness values (inhalable and respirable fractions) in the plastic limit were assumed to be zero (critical point F). The plastic limit was determined according to the procedure described in UNE 103104:1993.

4. Results and discussion

4.1. Characterisation and dustiness results

Table 8 details the particle size distribution, specific surface area, moisture content, bulk density, Hausner ratio, and dustiness data (inhalable and respirable mass fractions) obtained for each studied raw material and the corresponding test samples.

Table 8. Results of the physical characterisation and dustiness of the studied raw materials and test samples

Raw material	Particle physical characterisation					Bulk physical characterisation					
	PSD				^{B)} S (m ² /g)	Sample	Moisture content (%)	Bulk density (kg/m ³)	^{C)} HR	^{D)} Dustiness data	
	^{A)} d _i (µm)			d ₉₀ /d ₁₀						w _i (mg/kg)	w _R (mg/kg)
	d ₁₀	d ₅₀	d ₉₀								
C1	0.92	4.89	14.52	15.78	13.70	C1-1	0.08	598	1.63	19185	194
						C1-2	1.77	569	1.74	11986	107
						C1-3	2.42	606	1.65	13667	147
						C1-4	4.5	552	1.85	11635	80
						C1-5	5.52	604	1.71	15040	97
						C1-6	6.46	637	1.63	16258	87
						C1-7	7.43	668	1.57	10060	41
						C1-8	8.54	594	1.79	4266	3
						^{E)} C1-9	14	-	-	0	0
C2	1.04	5.8	19.19	18.45	32.97	C2-1	1.44	762	1.40	41433	445
						C2-2	3.04	699	1.55	34676	381
						C2-3	4.1	676	1.62	24352	353
						C2-4	4.92	713	1.55	29471	508
						C2-5	6.42	679	1.66	17766	164
						C2-6	7.64	712	1.60	27780	196
						C2-7	8.95	739	1.56	15147	19
						C2-8	9.59	699	1.66	5506	17
						^{E)} C2-9	14	-	-	0	0
C3	0.68	2.72	10.07	14.81	29.66	C3-1	0.26	398	2.04	30622	498
						C3-2	0.7	403	2.02	14995	140
						C3-3	1.80	384	2.15	14312	127
						C3-4	3.29	374	2.24	13832	83
						C3-5	4.69	382	2.22	15524	110
						C3-6	6.10	408	2.11	14573	94
						C3-7	7.80	491	1.79	12978	58
						C3-8	9.44	609	1.47	11997	53
						C3-9	13.99	657	1.43	6918	20
						^{E)} C3-10	25.00	-	-	0	0

Table 8. Results of the physical characterisation and dustiness of the studied raw materials and test samples

Raw material	Particle physical characterisation					Bulk physical characterisation					
	PSD				^{B)} S (m ² /g)	Sample	Moisture content (%)	Bulk density (kg/m ³)	^{C)} HR	^{D)} Dustiness data	
	^{A)} d _i (m)			d ₉₀ /d ₁₀						w _i (mg/kg)	w _R (mg/kg)
	d ₁₀	d ₅₀	d ₉₀								
K1	2.80	8.01	25.82	9.22	12	K1-1	0.33	545	1.87	17348	186
						K1-2	1.13	556	1.85	13390	75
						K1-3	2.38	594	1.76	21985	231
						K1-4	5.83	623	1.74	17211	116
						K1-5	7.9	670	1.65	18315	130
						K1-6	10.58	712	1.60	14288	69
						^{E)} K1-7	29	-	-	0	0

^{A)} d_i: diameter below which lies I% by volume of total particles

^{B)} S: specific surface area

^{C)} Hausner ratio

^{D)} w_i: inhalable mass fraction; w_R: respirable mass fraction

^{E)} Plastic limit

Figures 7 and 8 show the variation of inhalable and respirable mass fractions with moisture content.

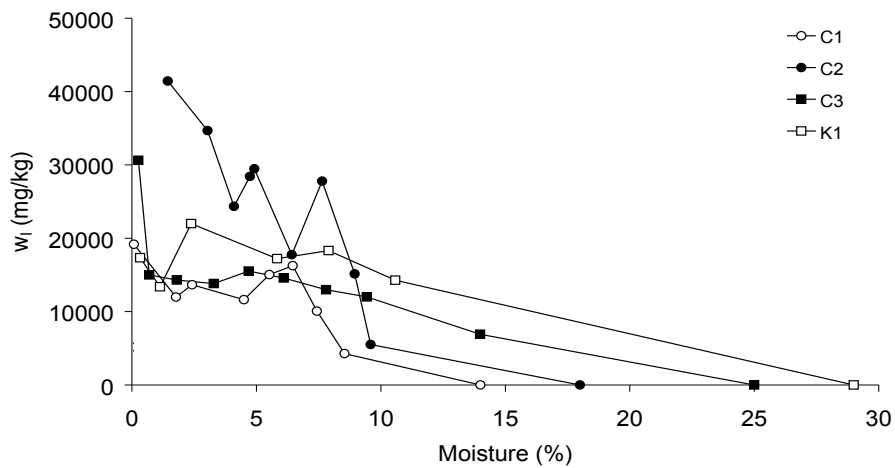


Figure 7. Variation of inhalable mass fraction with moisture content

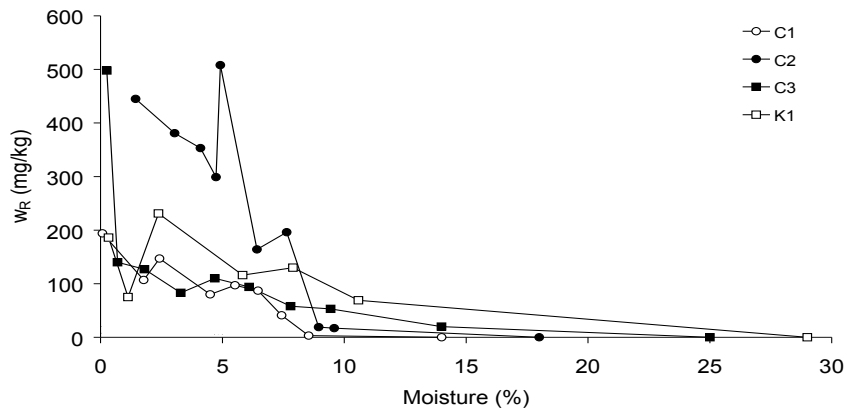


Figure 8. Variation of respirable mass fraction with moisture content

Figures 7 and 8 show that the effect of moisture on dustiness is quite complex. In fact, as against what might intuitively be expected, at intermediate moisture there were two stages in which dustiness rose with moisture.

4.2. Determination of the critical points by applying the developed methodology

The influence of the hydration mechanisms on dustiness was evaluated by using the methodology described above to identify the critical points or stages in the hydration process.

By way of example, Figure 9 shows the moisture adsorption isotherms for C1 and C2. Table 10 summarises the critical points obtained for the four studied materials.

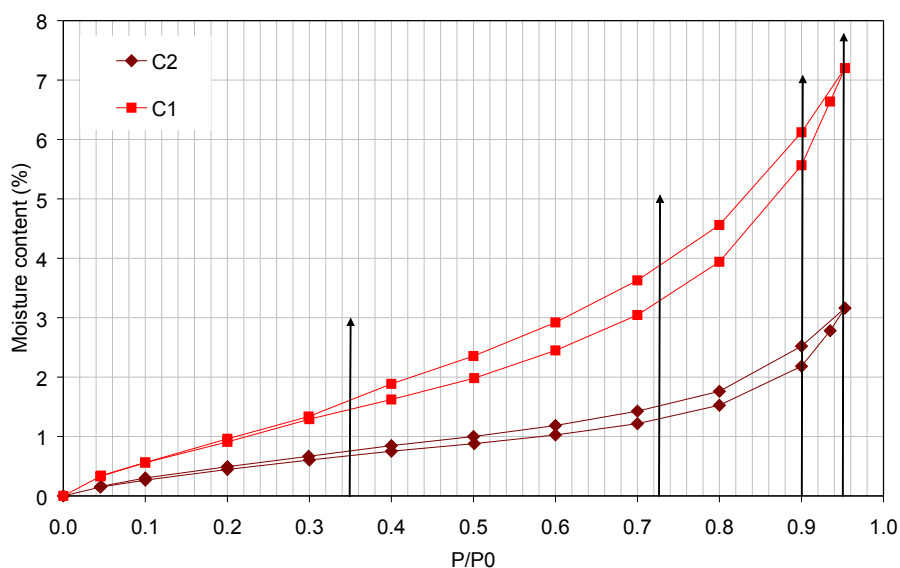


Figure 9. Moisture adsorption isotherms of C1 and C2

Table 9. Identification of the critical points in the C2 hydration process

Domain	Stage	Critical point	Moisture (%)				Description
			C1	C2	C3	K1	
1	Adsorption on hydrophilic sites	A	0.7	1.5	1.4	0.6	Monolayer (perturbed by the surface)
2	Multilayer adsorption	B	1.3	3.3	3.0	1.1	2 layers (perturbed by the surface)
		C	2.2	5.6	5.0	1.9	3 layers (perturbed by the surface)
		D	3.2	7.2	6.5	2.8	4 layers (not perturbed by the surface)
3	Capillarity condensation	E	7.0	7.7	8.7	7.1	Transition point between the pendular and the funicular state
4	Plastic limit	F	14.0	18.0	25.0	29.0	Transition to slurry state

4.3. Discussion of dustiness results based on the identified critical points

The critical points and variation of dustiness and Hausner ratio with moisture for the four studied raw materials are shown in figures 10 to 13.

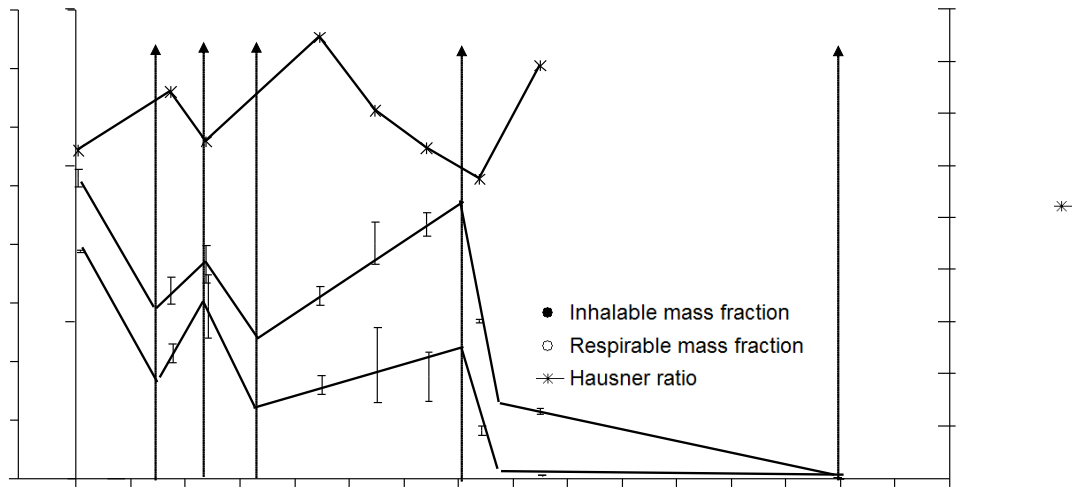


Figure 10. Critical points and variation of dustiness and Hausner ratio of C1

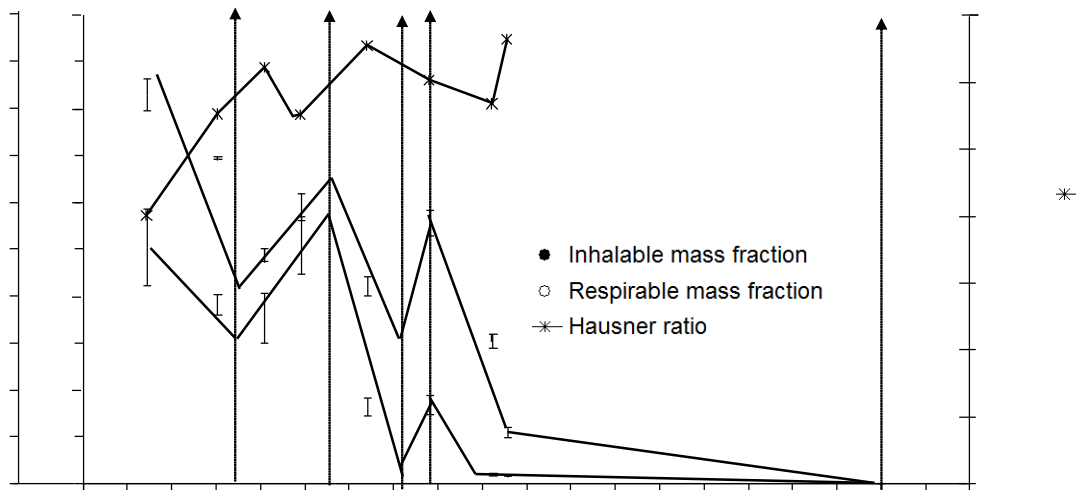


Figure 11. Critical points and variation of dustiness and Hausner ratio of C2

0-9-07 17

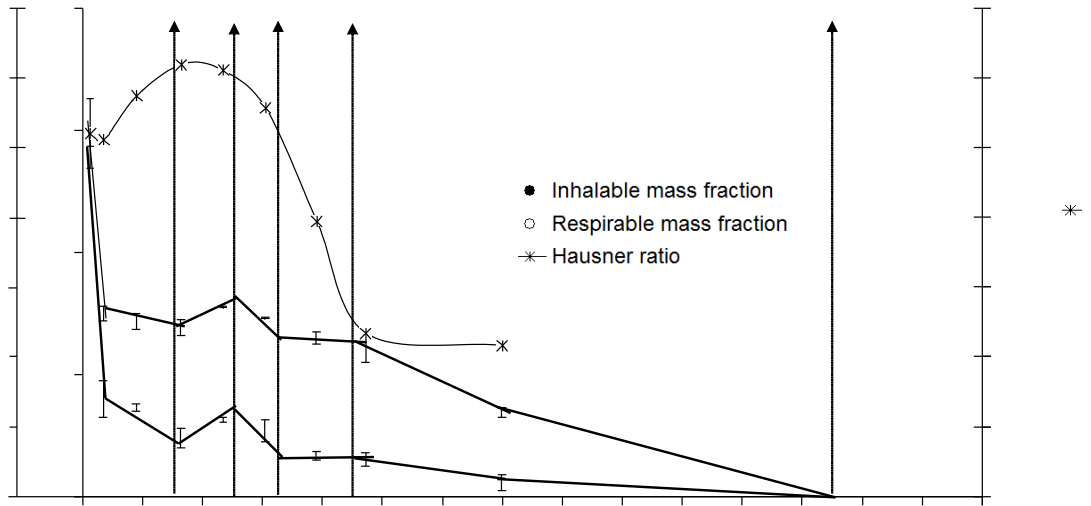


Figure 12. Critical points and variation of dustiness and Hausner ratio of C3

0-9-07 17

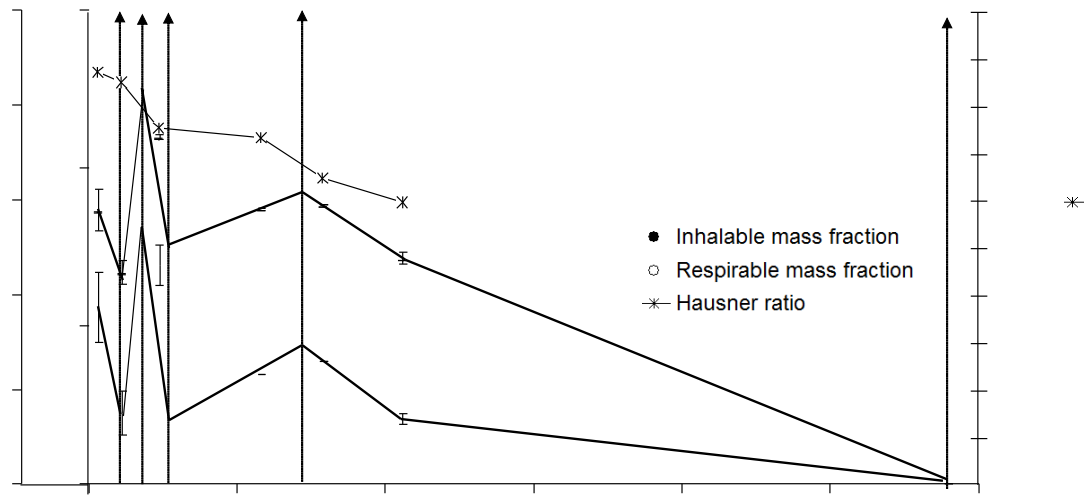


Figure 13. Critical points and variation of dustiness and Hausner ratio of K1

Figures 10 to 13 show that the calculated critical points exhibit good agreement with the experimental dustiness minimum and maximum values obtained for the studied raw materials. The critical points always appear to be the same for the studied materials, suggesting that the critical points are related to the different effect of water, depending on the mechanism involved. In the first stage, the added water (A→B) increased cohesion (raising the Hausner ratio and lowering dustiness) owing to the generation of liquid bridges, etc. However, as more water molecular layers formed (B→C), interparticle distance increased and interparticle attraction decreased (lowering the Hausner ratio and raising dustiness).

When more water was added (C→D), these water layers, which were not perturbed by the clay surface, presumably tended to stick particulate groups together, thus again increasing cohesion (raising the Hausner ratio and lowering dustiness).

However, when sufficient water was added to granulate the sample (D→E), flowability improved again (lowering the Hausner ratio and raising dustiness) owing to increased agglomerate size (Albaro et al., 1987; Amorós et al., 1986; Oliva, 2015). Dustiness maximised in this stage, as a function of the presence of free particles, particle size, and agglomerate size. Finally, when more water was added (E→F), though flowability improved, granulate strength increased about threefold (Oliva, 2015), constraining dust release during handling (funicular state) and thus reducing dustiness. Finally, from the capillary state on, cohesion increased and dustiness decreased until the latter became negligible (presumably at the plastic limit).

It may be noted that these results are consistent with previous studies in which the dustiness index of some materials rose when the moisture content increased slightly, the dustiness index then decreasing when moisture content increased further (Cowherd et al., 1989; Plinke et al., 1995).

Finally, though water adsorption isotherms were not examined in depth in the present study, the clay hydration mechanisms involved were observed to significantly influence the effect of moisture on dustiness. The results indicate that the effect of moisture was quite complex and depended not only on the material but also on water molecule location, which raised or lowered cohesion and therefore increased or decreased dustiness. This behaviour cannot be extrapolated directly to other materials because the effect of moisture depends on the material and on the material's surface properties and hygroscopicity (WHO/SDE/OEH/99.14). However, the methodology developed for the identification of the critical points from the water adsorption isotherm can help predict or better understand the effect of moisture on the dustiness of other clays or even on that of materials of different nature. The methodology may thus be considered general enough to be extrapolable to other types of materials.

4 Conclusions

In this study of the variation of dustiness of four clay materials with moisture content, as against what might intuitively be expected, the resulting behaviour was quite complex. The effect of moisture is known to depend on the material (WHO/SDE/OEH/99.14), but the results indicate that this also depends on whether the water acts as a binder or as a lubricant, i.e. it depends on water location.

To better understand the phenomena involved in the clay hydration process, a specific methodology was developed to estimate the critical points of the clay hydration process based on the water adsorption isotherm, saturation degree, and plastic limit.

The methodology used and the results obtained allowed the critical clay hydration points and their influence on the effect of moisture on dustiness to be identified. In this regard, as against what might intuitively be expected, this study suggests that intermediate moisture contents

might not significantly reduce clay dustiness, but could even raise dustiness (moisture content from critical point B to C and D to E). For this reason, only moisture contents above the critical point E (pendular–funicular transition point, 7–9% for the studied materials) assure low dustiness values, whilst at intermediate contents more attention should be paid.

From the occupational health point of view, the implementation of preventive and corrective measures based on clay wetting should be based on a specific study of the material. For instance, clay C2 show higher dustiness at 5% than at 3% of moisture. In this regard, the application of the developed methodology should allow the establishment of adequate process controls and/or abatement systems employed to minimise particulate matter exposure in workplaces and outdoors.

Finally, considering that the developed methodology is based on the mechanisms that take place during the hydration of powders, it should be highlighted that it can be readily applied to other types of clays or, more generally to different types of hygroscopic materials.

Acknowledgements

This work was supported by the Spanish Ministry of Science and Innovation (MINECO) through the research project “Prediction of emissions and exposure to micro and nanoparticles in industrial environments”; acronym PREDEXPIN, reference CGL2015-66777-C2-2-R. The project has been co-funded by the European Regional Development Fund (ERDF). The Generalitat Valenciana has also supported the work through a grant, reference (ACIF/2012/111), under the Vali+d Programme for trainee researchers and the project IMAMCA/2015/1, which has been financially supported by IVACE and the Comunidad Valenciana Operative Programme FEDER 2014-2020.

References

1. Albaro, J. A., Fuentes, A. B., Navarro, J. E., Medall, F. N., 1987. Características de polvos cerámicos para prensado. *Boletín de la Sociedad Española de Cerámica y Vidrio* 26, 31–37.
2. Alwis, U., Mandryk, J., Hocking, A. D., Lee, J., Mayhew, T., Baker, W., 1999. Dust exposures in the wood processing industry. *American Industrial Hygiene Association Journal* 60(5), 641–646.
3. Amorós, J. L., Negre, F., Felú, C., 1986. Método de determinación de las características tecnológicas de aglomerados. I. Métodos de determinación de la fluidez y de la densidad aparente. *Técnica Cerámica* 146, 380–386.
4. Benchara, A., 1991. Etats et localisation de l'eau retenue par des matériaux finement divisés. Mécanismes de l'hydratation et du gonflement-retrait [equation de Frenkel-Halsey-Hill, isotherme de desorption d'eau, adsorption multicouche, état condensé et adsorbe, courbes].
5. Carrott, P. J. M., McLeod, A. I., Sing, K. S. W., 1982. Application of the Frenkel-Halsey-Hill equation to multilayer isotherms of nitrogen on oxides at 77K. *Studies in surface science and catalysis* 10, 403–410.
6. Certificación AENOR, 1993. Determinación del límite plástico de un suelo (UNE 103104: 1993). [Spanish standard]
7. Cowherd, C., Grelinger, M.A., Englehart, P.J., Kent R.F., Wong, K.F., 1989. An apparatus and methodology for predicting the dustiness of materials. *Am. Ind. Hyg. Assoc. J.* 50, 123–30
8. European Committee for Standardization, 2013. Workplace exposure: measurement of the dustiness of bulk materials; Part 1: Requirements and choice of test methods; Part 2: Rotating drum method; Part 3: Continuous drop method (EN 15051). [Standard]

9. European Committee for Standardization, 1992. Workplace atmospheres. Size fraction definitions for measurement of airborne particles (EN 481). [Standard]
10. Farrugia, T. R., Ahmed, N., Jameson, G. J., 1989. A new technique for measuring dustiness of coal. *Journal of Coal Quality* 2, 55.
11. Haggymassy, J., 1970. Pore structure analysis by water vapor adsorption. Department of Chemistry, Clarkson College of Technology.
12. Hjemsted, K., Schneider, T., 1996. Documentation of a dustiness drum test. *Annals of Occupational Hygiene* 40(6), 627–643.
13. Instituto Geológico y Minero de España, IGME. Available from: <http://www.igme.es/> (accessed 14.12.16).
14. International Organization for Standardization, 2009: Particle Size Analysis: Laser Diffraction Methods. Part 1: General Principles (ISO 13320-1). [Standard]
15. IPTS, European Commission, 2006: Reference Document on Best Available Techniques on Emissions from Storage. Available from: <http://eippcb.jrc.ec.europa.eu/reference/> (accessed 14.12.16).
16. International Organization for Standardization, 2004. Fine ceramics (advanced ceramics, advanced technical ceramics) -- Determination of absolute density of ceramic powders by pycnometer (ISO 18753:2004).
17. International Organization for Standardization, 1995. Determination of the Specific Surface Area of Solids by Gas Adsorption using the BET Method (ISO 9277).
18. Leith, D., 1991. Fundamental factors that affect dust generation. NTIS, SPRINGFIELD, VA(USA).
19. López-Lilao, A., Bruzi, M., Sanfélix, V., Gozalbo, A., Mallol, G., Monfort, E., 2015. Evaluation of the dustiness of different kaolin samples, *Journal of Occupational and Environmental Hygiene* 12(8), 547–554.

20. López-Lilao, A., Escrig, A., Orts, M. J., Mallol, G., Monfort, E., 2016. Quartz dustiness: a key factor in controlling exposure to crystalline silica in the workplace. *Journal of occupational and environmental hygiene* 13(11), 817-28.
21. Mallol, G., Amoros, J.L., Orts, M.J., Llorens, D., 2008. Densification of monomodal quartz particle beds by tapping. *Chem. Eng. Sci.* 63, 5447–56
22. Moore, D. E., Lockner, D. A., 2007. Friction of the smectite clay montmorillonite. *The seismogenic zone of subduction thrust faults*, 317–345.
23. Mukherjee, S., Ghosh, B., 2013. *The science of clays*. India: Capital Publishing Company.
24. Oliva, M., 2015. Available from: <http://ocw.ub.edu/farmacia/tecnologia-farmaceutica-i/fitxers/temes/T.06-GRANULACIO.pdf> (accessed 14.12.16).
25. Ormerod, E. C., Newman, A. C. D., 1983. Water sorption on Ca-saturated clays: II. Internal and external surfaces of montmorillonite. *Clay Miner*, 18(3), 289–299.
26. Plinke, M.A.E., D. Leith, M.G. Boundy, Löffler, F., 1995. Dust generation from handling powders in industry. *The Am. Ind. Hyg. Assoc. J.* 56, 251–7.
27. Plinke, M. A., Maus, R., Leith, D., 1992. Experimental examination of factors that affect dust generation by using Heubach and MRI testers. *The American Industrial Hygiene Association Journal* 53(5), 325–330.
28. Prost, R., Koutit, T., Benchara, A., Huard, E., 1998. State and location of water adsorbed on clay minerals: consequences of the hydration and swelling–shrinkage phenomena. *Clays and clay minerals* 46(2), 117–131.
29. Revil, A., Lu, N., 2013. Unified water isotherms for clayey porous materials. *Water Resources Research* 49(9), 5685–5699.

30. Teschke, K., Marion, S. A., Vaughan, T. L., Morgan, M. S., Camp, J., 1999. Exposures to wood dust in US industries and occupations, 1979 to 1997. *American journal of industrial medicine* 35(6), 581–589.
31. Westborg, S., Cortson, C. E., 1990. Determination of dustiness of coal by rotating drum method. *Journal of Coal Quality* 9(3), 77.
32. World Health Organization, 1999. Hazard prevention and control in the work environment: airborne dust. WHO/SDE/OEH/99.14